Resonance-Driven Ultrasound-Assisted Germination of *Cucurbita pepo*: A Multiphysics-Based Process Intensification Approach

Daniel Aguilar-Torres *, Omar Jiménez-Ramírez, Felipe A. Perdomo, Rubén Vázquez-Medina *

Posted Date: 27 February 2026

doi: 10.20944/preprints202602.1926.v1

Keywords: ultrasound-assisted germination; multiphysics analysis; thermoacoustic effects; resourceefficient agriculture; energy- and water-saving

Article

Resonance-Driven Ultrasound-Assisted Germination of *Cucurbita pepo*: A Multiphysics-Based Process Intensification Approach

Daniel Aguilar-Torres [1,2,*], Omar Jiménez-Ramírez [3], Felipe A. Perdomo [4] and Rubén Vázquez-Medina [1,*]

[1] Instituto Politécnico Nacional, Centro de Investigación en Ciencia Aplicada y Tecnología Avanzada-Querétaro, Cerro Blanco 141, Colinas del Cimatario, Santiago de Querétaro, 76090,Querétaro, Mexico
[2] Secretaría de Ciencia, Humanidades, Tecnología e Innovación, Insurgentes Sur 1582, Crédito Constructor, Benito Juárez, 03940, CDMX, Mexico
[3] Instituto Politécnico Nacional, Escuala Superior de Ingeniería Mecánica y Eléctrica Unidad Culhuacan, Santa Ana 1000, San Francisco Culhuacan, Coyoacán, 04440, CDMX,Mexico
[4] Faculty of Engineering and Science, University of Greenwich, Central Avenue Chatham Maritime Kent ME4 4TB, U.K.
* Correspondence: dan_a_torres@hotmail.com, ruvazquez@ipn.mx

Abstract

Ultrasound-assisted germination (UAG) has been proposed as a process intensification strategy to enhance seed performance while improving resource efficiency. This study combines thermoacoustic multiphysics modeling with controlled experimental validation to evaluate resonance-driven UAG in *Cucurbita pepo*. Frequency-domain analysis identified 40 kHz as the resonance condition of the seed system, enabling localized acoustic energy concentration. Thermoacoustic simulations demonstrated that temperature increases remained below 46 °C across all exposure times, ruling out bulk thermal effects and supporting a predominantly mechanical activation mechanism associated with enhanced permeability and mass transfer. Experimental treatments (40 kHz, 1.5 MPa, 5–25 min) revealed a non-linear germination response to acoustic exposure. A 10 min treatment produced the optimal outcome, increasing final germination from 20% in untreated seeds to 47% and reducing the time required to reach steady state from 13 to 10 days. Longer exposure times did not generate proportional improvements, indicating the presence of a finite acoustic energy window beyond which diminishing returns occur. Because daily water (0.45 L·day^{-1}) and electrical (0.438 kWh·day^{-1}) consumption remained constant across treatments, the shortened germination period directly reduced cumulative resource demand. Under optimal conditions, total water consumption decreased by approximately 1.35 L and electricity use by 1.31 kWh per germination cycle relative to the control. When normalized per percentage point of germination achieved, energy and water intensity were reduced by nearly threefold. The integration of multiphysics modeling with biological experimentation establishes a mechanistically validated and energy-optimized framework for UAG, supporting its application in resource-efficient controlled-environment agricultural systems.

Keywords: ultrasound-assisted germination; multiphysics analysis; thermoacoustic effects; resource-efficient agriculture; energy- and water-saving

1. Introduction

Seed germination is a critical stage in plant development and agricultural production, directly influencing crop establishment, uniformity, and yield. Conventional approaches to enhance germination, such as chemical priming, thermal treatments, and mechanical scarification, are often limited by long processing times, high resource consumption, or potential environmental and physiological drawbacks [1–3]. In this context, physical process intensification techniques have gained increasing attention as sustainable alternatives for improving seed performance without chemical inputs.

 doi:10.20944/preprints202602.1926.v1

Among these techniques, ultrasound-assisted processing has emerged as a promising tool for enhancing seed germination and early seedling development. Ultrasound induces mechanical vibrations and pressure fluctuations in the surrounding medium, leading to phenomena such as cavitation, microstreaming, and enhanced mass transfer [4–6]. When applied to seeds, these effects can modify seed coat permeability, accelerate water uptake, and stimulate metabolic activity, ultimately improving germination kinetics and uniformity [7–9]. Recent studies have demonstrated that low- and moderate-intensity ultrasound treatments can significantly increase germination rate, reduce mean germination time, and promote seedling vigor across a wide range of plant species [10–12]. However, as highlighted in the comprehensive review by Nogueira *et al.* [13], the reported effects of ultrasound on germination are highly dependent on process parameters such as frequency, power density, exposure time, and treatment medium. Moreover, the lack of standardized experimental conditions and limited mechanistic understanding hinder the scalability and reproducibility of UAG processes.

From an engineering perspective, one of the main gaps identified in the literature is the insufficient characterization of the acoustic field and its interaction with biological materials. Most studies report nominal ultrasound parameters without accounting for spatial and temporal variations in acoustic pressure, energy distribution, or cavitation activity within the treatment system [14,15]. As a result, the relationship between acoustic conditions and biological responses remains largely empirical, limiting the rational design and optimization of UAG processes. In addition, few studies have approached UAG from a process engineering and intensification standpoint, integrating experimental observations with physical modeling or energy efficiency considerations [16,17]. These limitations can be addressed through a systematic analysis of ultrasound-matter interactions. This analysis should be supported by quantitative measurements and modeling tools that can describe the spatiotemporal behavior of the acoustic field and its effects on seed germination.

Therefore, the objective of this study is to contribute to the advancement of ultrasound-assisted seed germination by adopting an engineering-oriented approach that combines experimental evaluation with a detailed analysis of the acoustic process conditions. By doing so, this work aims to provide insights into the mechanisms governing ultrasound-induced enhancement of germination and to support the development of scalable, efficient, and reproducible ultrasound-based processes for agricultural applications.

In this context, *Cucurbita pepo* seeds were selected as a model system due to their agronomic relevance, well-documented physiological response during germination, and sensitivity to physical stimulation techniques. *Cucurbita pepo* is widely cultivated worldwide for food and agroindustrial applications, and its seeds are commonly used in both direct sowing and seedling production systems [18–20]. These characteristics make it an appropriate candidate for evaluating UAG from a process engineering perspective. Moreover, the relatively large seed size and robust seed coat facilitate experimental handling, reproducibility, and monitoring of germination dynamics. The insights obtained from this study are expected to contribute to the development of scalable UAG processes, with potential applicability at laboratory, pilot, and industrial scales, supporting seed treatment strategies for small-, medium-, and large-scale agricultural production systems.

1.1. Related works

A growing body of research has investigated ultrasound as a physical assistive technology to enhance seed germination and early seedling performance across diverse plant species. Pre-germination ultrasonic treatments have been shown to improve water uptake, partially disrupt seed coat barriers, and accelerate enzymatic activity, resulting in higher germination rates and increased seed vigor compared to untreated controls.In this context, Foschi *et al.* (2023) [21] analyzed the effects of high-intensity ultrasound on the imbibition and germination performance of *Capparis spinosa L.* seeds using an ultrasonic probe at different output powers and treatment durations. Ultrasonic stimulation accelerated the initial imbibition phase by inducing partial scarification of the testa while preserving the tegmen, allowing water uptake through the hilar region without altering seed viability. However, germination was highly sensitive to treatment intensity, showing a significant negative correlation with

 doi:10.20944/preprints202602.1926.v1

the temperature reached during sonication; temperatures above 40 °C almost completely inhibited germination. Among the tested conditions, the combination of 20 W for 60 s resulted in the highest germination percentage (up to 71.7%, on average) and was the only treatment that significantly improved germination compared to the control, highlighting the importance of optimizing ultrasound parameters to avoid thermal damage. Building on these findings, Qin *et al.* (2024) [22] investigated the application of ultrasound treatment to improve the malting performance of *Hordeum vulgare L.* varieties characterized by high grain hardness and restricted water uptake. These varieties exhibited elevated expression of abscisic acid biosynthesis genes (NCED1 and NCED2), reduced expression of gibberellin biosynthesis genes, and lower hydrolytic enzyme activities during germination compared with a standard malting cultivar. Ultrasound treatment enhanced water uptake and stimulated gibberellin biosynthesis gene expression, partially alleviating the physical and hormonal constraints associated with grain hardness and resulting in improved malting quality. Further evidence was provided by Gong *et al.* (2024) [10] evaluated the effects of variable-frequency ultrasound (20–40 kHz for 40 s) on *Zea mays* seed germination. Ultrasonic treatment increased germination percentage and radicle length by 10.4% and 230.5%, respectively, and significantly enhanced the activity of key hydrolytic enzymes, including acid protease, α-amylase, and β-amylase. Transcriptomic analysis revealed extensive differential gene expression associated with metabolic pathways and hormonal regulation, characterized by increased auxin and gibberellin levels and reduced abscisic acid content. Furthermore, ultrasonic-treated seeds exhibited improved germination and radicle growth under salinity, drought, and waterlogging conditions, indicating enhanced tolerance to abiotic stress during early developmental stages. Similarly, Ramos-Pacheco *et al.* (2025) [23] investigated UAG in *Chenopodium quinoa Willd* by evaluating ultrasound frequency, exposure time, and germination duration using a factorial experimental design. Germination was monitored at 48 and 72 h, including non-sonicated controls at both time points. Ultrasonic pretreatment significantly increased total phenolic content (up to 12%), flavonoids (24.5%), and antioxidant capacity (15%) after 72 h of germination, while reducing amylose content and increasing reducing sugars. Structural and thermal analyses revealed subtle modifications in starch and protein organization associated with increased thermal stability. Although germination time was the most influential factor, ultrasound acted as an abiotic stimulus by increasing cell permeability and promoting phenolic biosynthesis. Extending these findings, Rashid *et al.* (2025) [24] examined the impact of UAG on selenium-biofortified *Oryza sativa L.*, focusing on its interaction with subsequent drying processes. Ultrasound pretreatment induced microstructural modifications, including increased porosity and microchannel formation, which enhanced mass transfer and were associated with improved retention of phenolic compounds and antioxidant capacity in germinated grains. Total phenolic and flavonoid contents increased by up to 36% and 24%, respectively, depending on the drying method, while antioxidant activity was significantly enhanced. These results further support the role of ultrasound as an abiotic stimulus during germination that modifies grain structure and metabolism, with downstream benefits for phytochemical stability and functional quality. Moreover, dos Santos *et al.* (2026) [25] investigated ultrasound-assisted intermittent hydration as a pre-germinative treatment for *Moringa oleifera* seeds under saline and non-saline conditions. Seeds were exposed to ultrasound in a bath system for 50 or 60 min, with germination monitored over 168 h. The 50 min ultrasound treatment significantly reduced average germination time (>11.5%) and increased germination percentage (>12.1%) compared to the control. Ultrasound also enhanced radicle and seedling growth by 35.7% and 42%, respectively. Under salinity stress (150 mmol NaCl), ultrasound partially mitigated inhibitory effects, confirming its biostimulant role during early germination. Collectively, these studies demonstrate the potential of ultrasound as an effective physical and abiotic stimulus to enhance seed germination, early seedling performance, and stress tolerance across a wide range of plant species. However, despite the reported benefits, most previous research has focused on biological and physiological responses, while treating ultrasound largely as a black-box input. To date, there is a lack of systematic characterization of the ultrasonic signals applied to different seed types, which limits the ability to rationally optimize the process. In particular, the relationships between ul-

 doi:10.20944/preprints202602.1926.v1

trasound frequency, intensity, exposure time, and temperature at the seed level remain poorly defined. This knowledge gap restricts the development of efficient, reproducible, and scalable UAG protocols, underscoring the need for studies that integrate signal characterization with seed-specific responses to enable process optimization and improved germination outcomes.

From this perspective, several studies have specifically addressed the improvement of germination in *Cucurbita pepo*, a species of high agronomic relevance whose seeds often exhibit variable germination behavior. Previous research has mainly examined the physiological factors and responses associated with germination enhancement in *Cucurbita pepo*, providing a valuable biological framework for evaluating emerging technologies aimed at improving germination performance. In parallel, ultrasound has been applied to *Cucurbita pepo* seeds as a physical tool to enhance mass transfer during the extraction of bioactive compounds. Macedo *et al.* (2022) [26] demonstrated that ultrasound-assisted extraction facilitated the release of phenolic compounds and antioxidants from *Cucurbita pepo* seeds, evidencing its capacity to modify seed internal structure and permeability. Although not focused on germination, these findings support the potential relevance of ultrasound-induced physical effects in *Cucurbita pepo* seeds for germination-assisted applications. In addition, hormonal regulation has been shown to play a central role in *Cucurbita pepo* seed germination. Iglesias-Moya *et al.* (2023) [27] demonstrated that the ethylene-insensitive etr2b mutant germinated earlier than the wild type under both water and abscisic acid (ABA) treatments, exhibiting reduced sensitivity to ABA during radicle elongation and early seedling growth. Molecular and hormonal analyses revealed that the etr2b mutation downregulated ABA biosynthesis and signaling during seed imbibition and germination, resulting in reduced dormancy. These findings highlight the importance of ethylene–ABA crosstalk as a key physiological mechanism controlling germination performance in *Cucurbita pepo*. Likewise, Acila *et al.* (2024) [28] evaluated the effects of cadmium and copper on *Cucurbita pepo* seed germination and embryonic axis metabolism. Germination percentage remained high (93.33% $\pm$ 5%); however, seed vigor index, embryonic axis length, and dry weight were significantly reduced under metal exposure. Alterations in antioxidant metabolism and stress-related enzymatic activity indicated metal-specific and concentration-dependent responses. These results highlight that germination efficiency in *Cucurbita pepo* is strongly influenced by post-germinative growth and metabolic balance, particularly under abiotic stress. In this framework, recent studies on *Cucurbita pepo* have highlighted the strong sensitivity of seed germination to abiotic stresses. Irik and Bikmaz (2024) [29] demonstrated that salinity significantly impaired germination performance, causing a 16.1% reduction in germination percentage, a 15.5% increase in mean germination time, and pronounced losses in seedling vigor, evidenced by a 46.9% decrease in the seedling vigor index. In addition, membrane integrity was adversely affected under saline conditions, with ion leakage increasing by 33.9%, indicating stress-induced cellular damage. Collectively, these findings reinforce the relevance of *Cucurbita pepo* as a suitable model for evaluating strategies aimed at mitigating stress-related constraints on germination and early seedling establishment. Further evidence of hormonal regulation during germination was provided by Alonso *et al.* (2024) [30], who analyzed the crosstalk among ethylene (ET), jasmonate (JA), and abscisic acid (ABA) in Cucurbita pepo under control and salt stress conditions. Under optimal conditions, no significant differences were observed between the wild type and the JA-deficient mutant lox3a at the onset of germination, and both genotypes reached 50% germination at 32 h. However, as germination progressed, lox3a exhibited a lower germination rate at intermediate time points (48–120 h) and reached a significantly lower final germination percentage (73.2%) compared to the wild type (88.7%). These results confirm that JA acts as a positive regulator of germination, primarily influencing the completion and overall efficiency of the process rather than its initial onset. Under NaCl treatment, germination was reduced over time in both genotypes, with no significant differences in germination kinetics or final percentage between the wild type and lox3a, indicating that JA does not substantially modify germination sensitivity to salt stress.

While previous studies have shown that hormonal interactions play a key role in regulating seed germination under various conditions, these findings also highlight the potential benefits of

 doi:10.20944/preprints202602.1926.v1

complementary strategies to enhance early germination. In addition to endogenous hormonal regulation, physical priming approaches have emerged as promising non-chemical methods to improve germination efficiency by modifying the seed's structure and physiology. Among these, ultrasound has received increasing attention for its ability to enhance water uptake and stimulate early metabolic activity during germination. For instance, Liang et al. (2022) [31] investigated the combined optimization of ultrasound pre-treatment and germination in seven commercial seed-rich cultivars of *Cucurbita pepo* (LR-1, LR-2, LR-3, JH-4, RF-9, YH-3, and XC-2). Ultrasound was applied during seed soaking at a fixed frequency of 40 kHz, testing power levels of 100, 200, and 300 W with treatment durations of 10, 20, 30, and 40 min, while maintaining the processing temperature at approximately 30 °C. Under optimized conditions—generally around 300 W for 30 min, depending on the cultivar—seeds reached final germination percentages exceeding 90% within 72 h, accompanied by a reduction in mean germination time compared to untreated controls. The magnitude of the response varied among cultivars, indicating genotype-dependent sensitivity to acoustic intensity, which the authors attributed to ultrasound-induced microstructural alterations in the seed coat, improved water uptake dynamics, and stimulation of early metabolic processes during imbibition.

Building upon these findings, Pacheco *et al.* (2025) [32] further demonstrated that ultrasound applied in an intermittent manner during seed hydration can significantly enhance both hydration kinetics and germination performance in *Cucurbita pepo*. In their study, seeds were subjected to pulsed sonication (25 kHz, 38 W/L) for one to four cycles of 10 min during soaking at 25 or 45 °C, rather than continuous exposure. This strategy reduced hydration time by up to 54.3%, particularly when four cycles were applied at 45 °C, reflecting intensified mass transfer likely associated with cavitation-induced microstructural modifications of the seed coat. Regarding germination, ultrasound treatments shortened the lag phase (λ) by up to 11.7%, slightly increased maximum germination capacity (G_{max}) to approximately 95–97%, and reduced average germination time by up to 12.1% compared with non-sonicated controls. Although the intrinsic germination rate remained largely unaffected, sonicated seeds exhibited enhanced early vigor, as evidenced by greater radicle elongation (up to 19.4% increase), supporting the role of controlled intermittent ultrasound as a process-intensification strategy for improving germination dynamics in *Cucurbita pepo*.

Overall, the study of *Cucurbita pepo* germination has been approached through diverse physiological, biochemical, and environmental strategies, providing valuable insights into hormonal regulation, stress responses, and seed vigor enhancement. However, despite the promising outcomes reported for UAG, a substantial gap remains in establishing a rigorous theoretical framework to guide the rational application of ultrasonic stimulation. Many experimental studies, although demonstrating significant improvements in germination percentage, hydration kinetics, and early seedling growth, treat ultrasound primarily as an empirical input rather than as a controllable physical signal. In particular, limited attention has been given to the systematic characterization and optimization of key acoustic parameters, including stimulation frequency, acoustic pressure amplitude, and the temperature gradients generated within the propagation medium and at the seed level. A deeper understanding of these interrelated physical variables is essential to maximize process efficiency while preventing thermal or mechanical damage. Therefore, the present work focuses on the estimation and analysis of these critical ultrasonic parameters, aiming to establish a more mechanistically grounded and optimized approach to UAG in *Cucurbita pepo*.

1.2. Contribution of the Study

A mechanistically supported and quantitatively validated framework for UAG in large-seeded crops is established through the integration of thermoacoustic multiphysics modeling and controlled biological experimentation. In contrast to prior investigations predominantly based on empirical parameter screening—often limited to small-seeded species—the present work implements a resonance-based optimization strategy in *Cucurbita pepo*, linking frequency-domain analysis with germination kinetics.

 doi:10.20944/preprints202602.1926.v1

The principal contribution resides in the identification of 40 kHz as a resonance condition that promotes spatial localization of acoustic energy within the seed–fluid system while maintaining temperatures below critical thermal thresholds. The developed modeling framework enables prediction of acoustic pressure distribution and transient temperature fields, thereby reducing reliance on trial-and-error experimentation and providing a transferable methodology for other biological matrices.

Experimental validation reveals the existence of a finite acoustic energy window, with 10 minutes at 40 kHz and 1.5 MPa emerging as the optimal exposure condition. This treatment enhances germination efficiency, accelerates steady-state attainment, and decreases cumulative water and electrical consumption. The observed non-linear biological response to extended exposure underscores the necessity of energy-normalized optimization rather than prolonged sonication.

By quantitatively coupling acoustic energy localization, biological performance, and resource-intensity metrics, UAG is reframed from an empirical enhancement technique to a rationally designed process intensification strategy. The proposed modeling–validation approach establishes a reproducible pathway for optimizing acoustic pre-treatments.

Consequently, this paper is organized as follows. Section 2 describes the seed material, the mathematical formulation of the thermoacoustic model, and the multiphysics simulation framework used to characterize ultrasound–seed interactions. It further details the ultrasound treatment setup, controlled germination conditions, performance assessment criteria, and the methodology employed to quantify water and electrical energy consumption. Section 3 presents the numerical outcomes of the thermoacoustic simulations, the baseline germination behavior of untreated seeds, and the response under ultrasound-assisted treatments. Additionally, it provides a quantitative analysis of resource consumption across all experimental conditions. Section 4 interprets the results within a process-intensification and sustainability framework, examining the resonance-driven optimization strategy, the existence of a finite acoustic energy window, and the implications for energy-normalized process design. Finally, Section 5 summarizes the principal findings, highlights the methodological contributions, and outlines perspectives for scaling and further structural and techno-economic analyses.

2. Materials and Methods

2.1. Seed Material

The biological material selected for this study consists of seeds from *Cucurbita pepo*, a species encompassing agronomically important cultivars such as pumpkin, squash, and zucchini. These seeds are orthodox, dicotyledonous structures with a flattened, ovate morphology and a smooth, beige-colored seed coat. Internally, they contain a fully developed embryo and nutrient-rich cotyledons, predominantly composed of lipids and proteins, which support early metabolic activation during germination. The seed coat plays a critical role in regulating water permeability and protecting the internal tissues from mechanical and environmental stress.

The seeds used in this study were sourced from *El Trébol S.A. de C.V.*, a certified seed supplier based in Mexico. The batch, identified as STAC-2024, was provided with a declared purity of 99% and treated with thiram, a fungicidal agent commonly used to prevent seed-borne and soil-borne fungal infections during early germination. The high purity and standardized treatment ensure consistency in physiological response and minimize confounding biological variability during acoustic stimulation trials. From a physiological standpoint, *Cucurbita pepo* seeds exhibit high sensitivity to external stimuli, including temperature, moisture, and mechanical perturbations. This responsiveness makes them particularly suitable for evaluating innovative germination enhancement strategies based on ultrasound signals. In this context, acoustic stimulation via ultrasound signals aims to accelerate water uptake, disrupt dormancy mechanisms, and promote uniform metabolic activation. The interaction between ultrasound signals and seed tissues involves complex mechanical and thermal phenomena, which must be critically understood to optimize treatment protocols and predict germination outcomes.

 doi:10.20944/preprints202602.1926.v1

To support simulation and experimental analysis, a detailed physical characterization of the seeds is required. Specifically, the following parameters are considered: elastic modulus (E), speed of sound propagation (c_s), acoustic impedance (Z_s), density (ρ), thermal conductivity (k_s), specific heat capacity (C_{ps}), and geometric dimensions (length (l), width (w), and height (h)). These properties govern the transmission, absorption, and mechanical response of the seed matrix to ultrasound signals, and are therefore essential for modeling acoustic-thermal coupling phenomena. Table 1 presents the average values adopted for *Cucurbita pepo* seeds, based on relevant literature and targeted experimental measurements.

Table 1. Physical parameters of *Cucurbita pepo* seeds used for UAG modeling.

Species	ρ [kg/m^3]	c_s [m/s]	E [MPa]	Z_s [kPa·s/m]	α	l [mm]	w [mm]	h [mm]	k_s [W/m·K]	C_{ps} [kJ/kg·K]
Cucurbita pepo	1152.00	201.29	46.65	125.71	0.90	16.10	8.40	2.93	0.50	2000.00

Additionally, the seeds shown in Figure 1 correspond to the batch used in the UAG experiments described in this study.

Figure 1. *Cucurbita pepo* seeds used in the experimental procedure of UAG. The reddish coloration is due to thiram treatment applied by the seed distributor.

2.2. Mathematical Modeling

To simulate the propagation of ultrasound signals within *Cucurbita pepo* seeds, the classical linear wave equation (Eq. 1) was solved using the finite element method (FEM), following the formulation established by Blackstock *et al.* [33]. This equation governs the behavior of acoustic waves in heterogeneous media, including aqueous environments and biological tissues such as seed matrices:

$$c^2 \nabla^2 u - \frac{\partial^2 u}{\partial t^2} = 0 \,, \tag{1}$$

where u denotes the ultrasound pressure field, c is the speed of sound in the medium, t is time, and ∇^2 is the Laplacian operator applied to the spatial coordinates of $u(x, y, z)$. This formulation assumes linear, lossless propagation, which is valid for low-intensity ultrasound regimes typically used in germination studies.

A simplified two-dimensional geometry was constructed to resolve the acoustic field: the transmission medium (water) was modeled as a rectangular domain, while the seed was represented as an elliptical inclusion. Figure 2 illustrates the spatial configuration and boundary conditions applied.

 doi:10.20944/preprints202602.1926.v1

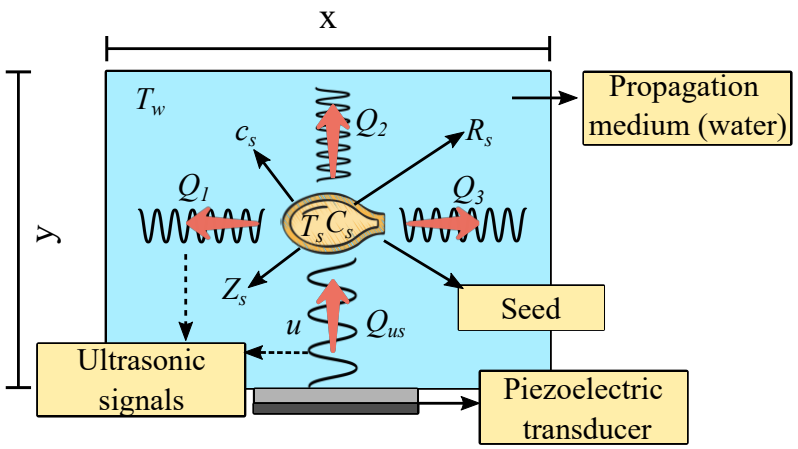

Figure 2. Simulation geometry for the thermoacoustic modeling of *Cucurbita pepo* seeds.

Based on the defined geometry and wave equation, the model computes the spatio–temporal distribution of ultrasound signals as they propagate through the medium and interact with the seed. Key acoustic properties such as impedance mismatch, absorption coefficient, and density gradients are incorporated to capture realistic wave–tissue interactions. To extend the analysis beyond mechanical stimulation, a thermal model was coupled to the acoustic field, treating ultrasound signals as localized heat sources that modulate the internal temperature of the seed. This approach enables the prediction of thermo–acoustic effects, which are relevant for evaluating safe and effective germination conditions.

The thermal behavior of the seed under ultrasound exposure is described by Eq. 2, adapted from Aguilar *et al.* [34,35]. This equation models transient heat transfer within the seed, incorporating both the input heat flux (Q_{us}) generated by ultrasound and the output fluxes (Q_1, Q_2, Q_3) representing dissipation to the surrounding medium:

$$\frac{\partial T_s}{\partial t} = \frac{\alpha P}{\rho_s C_{ps} A}\frac{\partial \bar{\varepsilon}}{\partial t} - \frac{3k_s}{\rho_s C_{ps} e}\nabla T_f \,, \tag{2}$$

where α is the local acoustic absorption coefficient, P is the pressure amplitude of the ultrasound signal, $\bar{\varepsilon}$ is the particle velocity, ρ_s is the seed density, C_{ps} is the specific heat capacity, A is the transverse area, k_s is the thermal conductivity, and ∇T_f is the temperature gradient between the seed (T_s) and the surrounding fluid (T_w).

The energy balance is governed by the relation $Q_{net} = \sum Q_{in} - \sum Q_{out}$, where:

- $\sum Q_{in} = Q_{us} = 2\alpha I = 2\alpha P \frac{\partial \bar{\varepsilon}}{\partial t}$, with $I = P\frac{\partial \bar{\varepsilon}}{\partial t}$ representing the local acoustic intensity.
- $Q_1 = Q_2 = Q_3 = \frac{1}{R_s}(T_s - T_w)$, with $R_s = \frac{e}{k_s}$ as the thermal resistance and $e = \Delta V$ the seed volume.
- $\sum Q_{out} = Q_1 + Q_2 + Q_3 = \frac{3}{R_s}(T_s - T_w)$.
- $C_s = \rho_s C_{ps} A$ is the thermal capacitance of the seed.

Under initial equilibrium conditions ($T_s = T_w$ at $t = 0$), only the ultrasound-induced flux Q_{us} is active, and no temperature gradient is present, highlighting the onset of thermoacoustic energy deposition. The right-hand terms of Eq. 2 thus represent the competing heat fluxes entering and leaving the seed system.

By integrating Eqs. 1 and 2, spatiotemporal simulations were performed using the thermophysical properties of *Cucurbita pepo* seeds. These simulations revealed localized temperature elevations within the seed and surrounding fluid, offering mechanistic insight into how ultrasound signals modulate thermal behavior. This coupled modeling framework supports the use of ultrasound as a non-invasive, energy-efficient strategy to influence seed physiology and enhance germination performance. A detailed analysis of ultrasound–seed interactions is presented in Section 3.

 doi:10.20944/preprints202602.1926.v1

2.3. Multiphysics Simulation Considerations

- **Software used:** Simulations were performed using COMSOL Multiphysics®, employing the *Pressure Acoustics* and *Heat Transfer* interfaces. These modules were coupled to resolve acoustic wave propagation and thermo–acoustic energy deposition within the seed.
- **Geometry and mesh configuration:** A 2D rectangular domain was defined to represent the water-filled germination chamber. A piezoelectric transducer with a diameter of 5 cm was placed at one boundary to emit ultrasound signals. The seed was modeled as an elliptical inclusion centered within the domain. Mesh resolution was set to $h = \lambda/10$ [36].
- **Boundary conditions and physical models:** The transducer boundary was defined as a harmonic pressure source with amplitude $P = 1.5$ MPa and frequency $f = 40$ kHz. Non-reflective boundary conditions were applied elsewhere to minimize artificial reflections. The acoustic field was resolved using the classical wave equation, while the thermal field was governed by a heat transfer model incorporating ultrasound-induced flux as a volumetric source.
- **Simulation parameters:** Water properties were defined as: speed of sound $c_w = 1480$ m/s, density $\rho_w = 998$ kg/m^3, and acoustic absorption coefficient $\alpha_w = 0.002$ Np/m. Seed properties were defined according to Table 1. A temperature threshold of 60 °C was imposed to prevent thermal damage and ensure physiological viability.

2.4. Ultrasound Treatment Setup

Ultrasound-assisted germination was performed using a benchtop ultrasonic bath (VEVOR, USA) with a working volume of 1.5 L, operating at a fixed frequency of 40 kHz and an acoustic pressure of 1.5 MPa. These conditions were selected based on the outcomes of the multiphysical analysis presented in Section 3, which identified optimal sonication parameters to enhance seed water imbibition and early metabolic activity without causing structural damage. Although the bath can reach temperatures up to 80 °C, the water level was maintained constant throughout all experiments to ensure uniform ultrasonic energy distribution and reproducible treatment conditions.

Cucurbita pepo seeds were fully submerged and subjected to one of five sonication durations: 5, 10, 15, 20, or 25 min. These times were selected to explore a range of exposure sufficient to induce microstructural modifications in the seed coat while minimizing potential stress or overheating effects. Each treatment was performed in quintuplicate to ensure statistical robustness. Immediately after sonication, seeds were transferred to standard germination conditions.

A control group, subjected to identical immersion and handling without ultrasound, was included to isolate the specific effects of ultrasonic treatment on germination performance and subsequent physiological responses. By maintaining consistent sonication parameters, immersion conditions, and post-treatment handling, this setup allowed for a reproducible evaluation of the influence of ultrasound on seed germination dynamics.

2.5. Germination Conditions

Germination experiments were conducted in a controlled growth chamber (VIVOSUN, USA; 50.8 × 35.5 × 53.3 cm), providing a stable environment to evaluate the physiological effects of ultrasound treatment independently of external factors. A full-spectrum LED lighting system maintained a 16 h light / 8 h dark photoperiod, simulating favorable diurnal conditions, while an internal blower ensured homogeneous air circulation throughout the chamber. The chamber temperature and relative humidity were maintained at approximately 25 ± 1 °C and 60–65%, respectively, providing stable and uniform conditions for seed germination.

Each treatment consisted of 5 replicates, with 30 seeds per replicate, germinated using a rinse-based method without substrate. Seeds were considered germinated when both cotyledons were fully exposed, and the process was followed until the germination rate reached a steady state. Periodic hydration ensured that seeds remained fully imbibed and properly oxygenated throughout the experiment, while uniform placement prevented localized microclimatic variations.

 doi:10.20944/preprints202602.1926.v1

These controlled conditions ensured reproducible and consistent environments, allowing observed differences in germination performance to be attributed primarily to the applied experimental treatments.

2.6. Ultrasound-Assisted Germination Setup

After the application of the ultrasonic pre-treatments and the inclusion of a non-sonicated control, seed germination was carried out using a custom-designed automated system to ensure process control and reproducibility. The system was developed to ensure precise regulation of hydration, illumination, and energy input during the germination stage. All structural components were fabricated from biodegradable polyethylene terephthalate (PET), providing mechanical stability and structural integrity.

The germination unit consists of a 20 cm $\times$ 23 cm $\times$ 10 cm water tank with a maximum capacity of 4 L. The tank is connected to a rinse module composed of a 20 cm $\times$ 23 cm $\times$ 5 cm tray designed to facilitate controlled hydration cycles. The tray includes three 2.5 mm diameter perforations that allow water to drain back into the tank, ensuring continuous recirculation. Inside the tray, a 15.5 cm $\times$ 22.5 cm drainer (3 cm height) contains twelve individual cavities (4 cm $\times$ 4 cm each) for seed placement, providing an effective germination area of 192 cm^2. Additionally, 1 mm^2 perforations distributed across the tray surface enable efficient drainage and prevent water accumulation, thereby reducing the risk of hypoxic conditions.

Illumination was provided by 22 W LED lamps programmed to maintain the established photoperiodic cycles required for germination. The automated hydration system incorporates a 3 W water pump responsible for recirculating water from the tank to the rinse tray. To maintain adequate seed hydration while ensuring proper oxygen availability, the pump operated under alternating cycles of 30 minutes ON and 30 minutes OFF. This intermittent regime promoted sustained moisture levels during imbibition while preventing prolonged submersion that could compromise gas exchange.

The complete system was implemented in experiments designed to quantify both water and energy consumption associated with the germination process, allowing an integrated evaluation of germination performance and process efficiency under controlled conditions. Figure 3 illustrates the germination system employed during the *Cucurbita pepo* germination assays, as well as the germination chamber used to maintain the controlled environmental conditions throughout the experimental period.

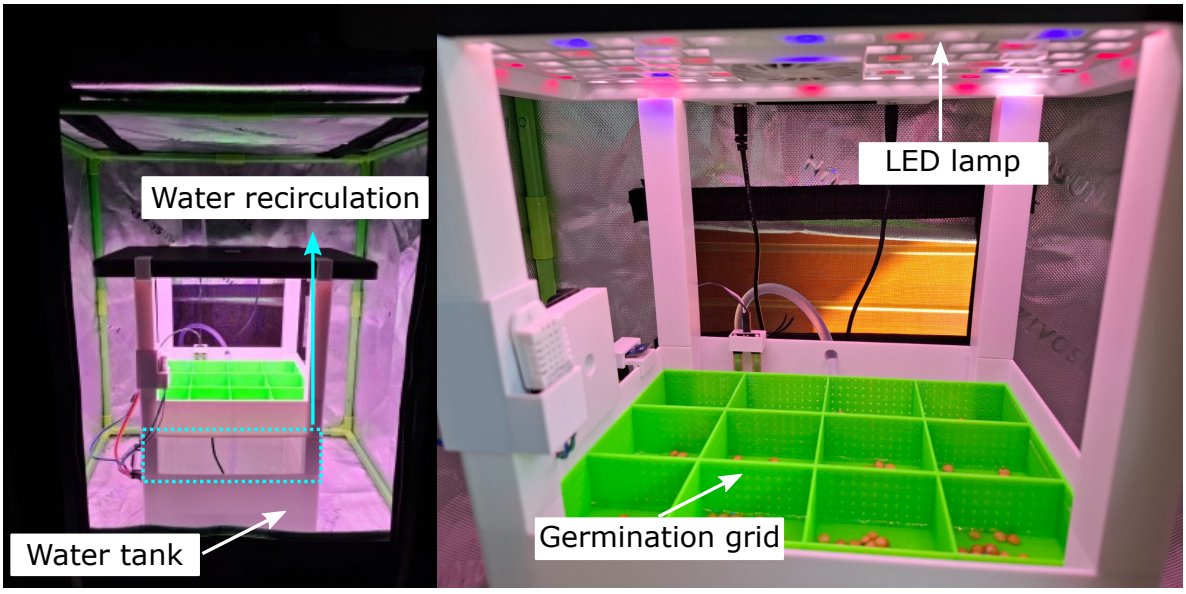

Figure 3. Experimental germination setup for *Cucurbita pepo*, including the water recirculation tank, automated intermittent hydration system, biodegradable PET germination grid, and LED-based photoperiod control inside the environmental chamber.

 doi:10.20944/preprints202602.1926.v1

2.7. Germination Performance Assessment

Germination performance was evaluated using quantitative indicators to ensure objective and reproducible assessment of seed behavior under the different experimental conditions. Two primary parameters were determined: germination rate (G_r) and germination index (G_i), which provide complementary information regarding germination capacity and temporal dynamics [37,38].

Each treatment consisted of five independent replicates of 30 seeds each (150 seeds per treatment). Germination was monitored at 24 h intervals under controlled environmental conditions. Germination rate (G_r) was calculated as the percentage of *Cucurbita pepo* seeds that successfully germinated relative to the total number of seeds tested. A seed was considered germinated when the cotyledons were visibly emerged, according to the predefined viability criteria established for this study.

The germination rate (G_r) was calculated according to Eq. 3:

$$G_r = \frac{G_s}{T_s} \tag{3}$$

where G_s is the total number of germinated seeds and T_s is the total number of seeds evaluated per treatment. Results were expressed as percentage values.

The germination index (G_i) was calculated according to Eq. 4:

$$G_i = \sum \left(\frac{G_t}{t} \right) \tag{4}$$

where G_t represents the number of seeds germinated on day t, and t corresponds to the time of observation (days). This index assigns greater weight to seeds that germinate earlier, thereby reflecting differences in germination speed and uniformity among treatments.

All measurements were performed simultaneously for ultrasound-treated and control groups to ensure direct comparability of germination dynamics.

2.8. Energy and Water Consumption Assessment

A comparative assessment of energy and water consumption was conducted to evaluate the operational efficiency of UAG of *Cucurbita pepo* relative to conventional (control) germination. The analysis quantified direct resource inputs under identical environmental conditions for the complete germination cycle.

Water consumption was determined by measuring the total volume of water used per germination unit (batch basis) throughout the entire germination period. This included the initial soaking stage and the automated hydration cycles applied during seed development. For ultrasound-treated samples, water use corresponded to the full post-treatment germination process, while control samples followed the same hydration protocol without ultrasonic exposure. Total water consumption was recorded per experimental run and expressed as the arithmetic daily mean over the duration of the germination cycle.

Energy consumption was directly measured using a calibrated power meter connected to the system. The total energy input (E) was recorded in kilowatt-hours (kWh) for the complete experimental run (batch basis), covering the entire germination cycle. Measurements included the electrical consumption of the ultrasonic device during treatment, as well as the 3 W water recirculation pump and the 22 W LED illumination system, which operated under identical programmed conditions for both treated and control groups. Baseline environmental conditions were maintained constant to ensure comparability. Energy consumption values were subsequently expressed as the arithmetic mean per day over the full germination period. This framework enabled a direct comparison of resource consumption between ultrasound-assisted and conventional germination processes under controlled operating conditions.

 doi:10.20944/preprints202602.1926.v1

3. Results

3.1. Thermoacoustic Simulation of Ultrasound—Seed Interaction

In the initial stage of the multiphysics simulation, the resonance frequency of Cucurbita pepo seeds was determined through a frequency-domain spectral analysis. To this end, a frequency sweep was performed over a bandwidth ranging from 20 to 50 kHz using an ultrasonic source delivering an acoustic pressure amplitude of 550 Pa. This pressure level was arbitrarily selected solely for resonance identification purposes and does not correspond to the operational conditions used in the experimental treatments. The spectral analysis revealed that the frequencies exerting the greatest influence on the mechanical response of the seed were concentrated within the 35–40 kHz range. Within this ultrasonic bandwidth, 40 kHz exhibited the highest response amplitude, and was therefore identified as the resonance frequency of the Cucurbita pepo seed. The resulting spectral response is presented in Figure 4, where the resonance peak at 40 kHz can be observed.

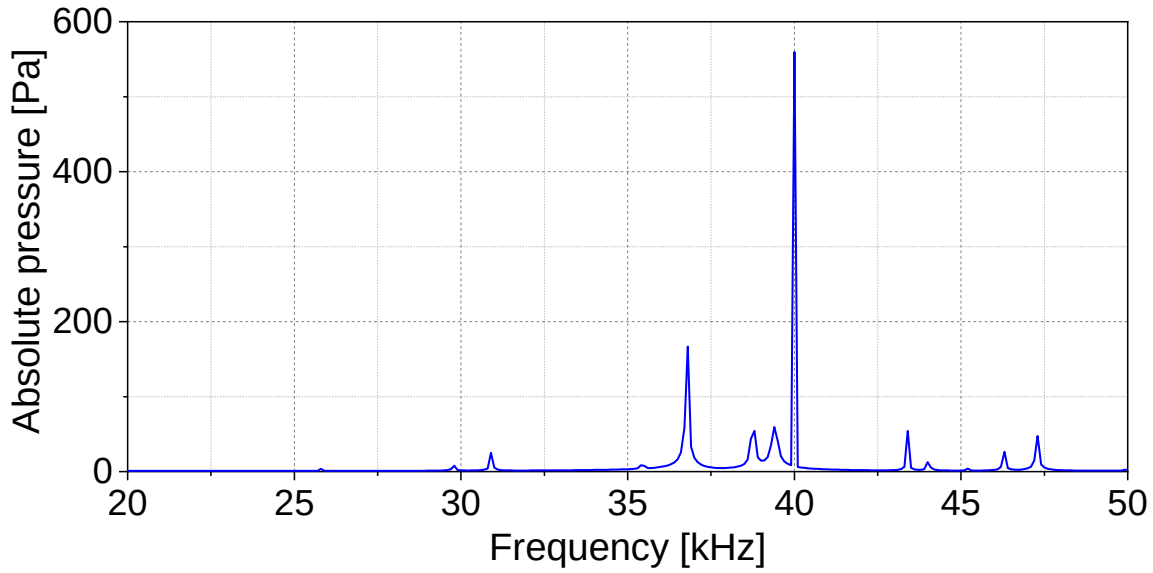

Figure 4. Spectral analysis of *Cucurbita pepo* seeds showing 40 kHz as the dominant resonance frequency.

Following the spectral analysis and the identification of 40 kHz as the resonance frequency of *Cucurbita pepo* seeds, a spatial analysis of the acoustic field was conducted at this frequency. The simulation incorporated the average seed dimensions reported in Table 1 to ensure geometric representativeness of the biological material. For this stage, the acoustic source was defined with a pressure amplitude of 1.5 MPa ($\sim$ 244 dB @1μPa) in order to maintain consistency with the operational conditions of the ultrasonic bath employed in the experimental trials.

The acoustic field distribution was evaluated through both two-dimensional (2D) and three-dimensional (3D) models to achieve a comprehensive visualization of ultrasound propagation and acoustic–structure interaction within the system. This approach enabled detailed characterization of pressure gradients and energy localization patterns at the resonance frequency. The spatial distribution of the acoustic field at 40 kHz is presented in Figure 5.

 doi:10.20944/preprints202602.1926.v1

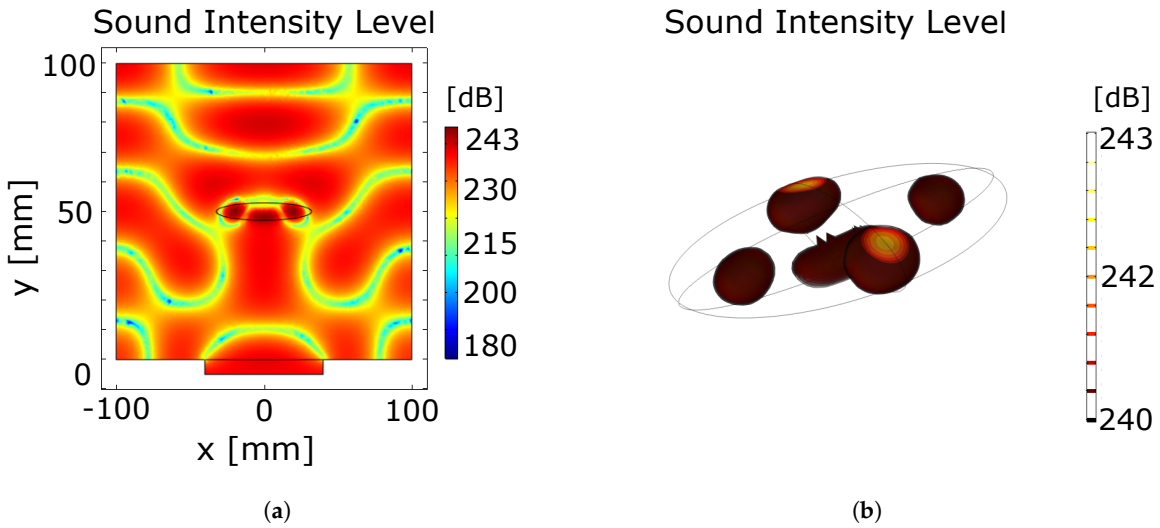

(**a**) (**b**)

Figure 5. Spatial localization of the acoustic field at 40 kHz within the ultrasonic system. (a) 2D intensity distribution; (b) 3D acoustic energy concentration in the seed structure.

The spatial distribution of the acoustic field at the identified resonance frequency (40 kHz) reveals a non-uniform pressure pattern characterized by the formation of well-defined pressure nodes and antinodes within the system. As shown in Figure 5(**a**), the two-dimensional sound intensity map exhibits alternating regions of high and low acoustic pressure resulting from constructive and destructive wave interference under resonant conditions. The maximum sound pressure level reaches approximately 243 dB, while adjacent regions display comparatively lower intensity values, thereby generating pronounced spatial pressure gradients. This structured distribution is indicative of standing wave formation, where nodal and antinodal regions define zones of minimum and maximum acoustic energy concentration, respectively. The presence of these pressure nodes is particularly relevant, as they create microdomains of intensified mechanical stimulation on the seed surface. At 40 kHz, the acoustic field does not distribute uniformly; instead, energy becomes spatially concentrated, enhancing localized stress and oscillatory loading on specific regions of the seed coat. Such localized pressure amplification increases the likelihood of microstructural perturbations in the testa, potentially facilitating enhanced water permeability and accelerating imbibition processes—critical early steps in seed germination.

The three-dimensional representation shown in Figure 5(**b**) further confirms the spatial localization of acoustic energy around and within the seed geometry. The 3D model illustrates discrete high-intensity nodes, with pressure levels ranging between approximately 240 and 243 dB, distributed across different regions of the seed structure. These nodes correspond to nodal regions of maximum acoustic pressure, where mechanical energy transfer from the ultrasonic field to the biological material is most efficient. Importantly, the distribution of these high-intensity zones is not confined to the external surface; rather, the acoustic coupling enables partial penetration and internal field modulation, suggesting volumetric mechanical stimulation. From a mechanistic standpoint, this resonance-driven concentration of acoustic energy supports a controlled stimulation regime, wherein energy delivery is maximized at specific structural locations without requiring indiscriminate increases in global pressure. The formation of pressure nodes and antinodes at 40 kHz therefore represents a physically optimized condition for UAG, as it promotes targeted mechanical activation.

Collectively, the 2D and 3D analyses demonstrate that excitation at the resonance frequency enhances acoustic field localization, increases pressure amplitude within defined microregions, and establishes spatially structured stimulation patterns.

To further quantify the spatial localization of the acoustic field at the resonance frequency, the sound intensity level (SIL) distribution was evaluated along a linear path across the system, as shown

 doi:10.20944/preprints202602.1926.v1

in Figure 6. This line was defined perpendicular to the central axis of the model, extending from the base of the ultrasonic transducer, traversing the geometric center of the *Cucurbita pepo* seed, and terminating at the boundary of the transmission medium (water domain). This approach enables a one-dimensional characterization of pressure amplitude variations along the principal axis of acoustic propagation.

As illustrated in Figure 6, the maximum acoustic intensity (SIL_{max}) reaches approximately 243 dB at a position located around 55 mm along the evaluated length. Notably, this peak corresponds spatially to the domain representing the seed, consistent with the seed position depicted in Figure 5(**a**). The coincidence between the resonance frequency (40 kHz) and the location of the maximum pressure amplitude within the biological domain provides strong evidence of effective acoustic–structure coupling under these operating conditions.

The profile further reveals oscillatory behavior characterized by alternating high- and low-intensity regions, reflecting the presence of pressure nodes and antinodes generated by standing wave formation. However, the dominant energy concentration occurs within the seed domain, confirming that resonance at 40 kHz promotes preferential energy localization in the biological material rather than in the surrounding aqueous medium. This spatial amplification within the seed structure substantiates the mechanistic role of resonance in maximizing mechanical stimulation, thereby reinforcing the suitability of 40 kHz as the optimal frequency for UAG enhancement.

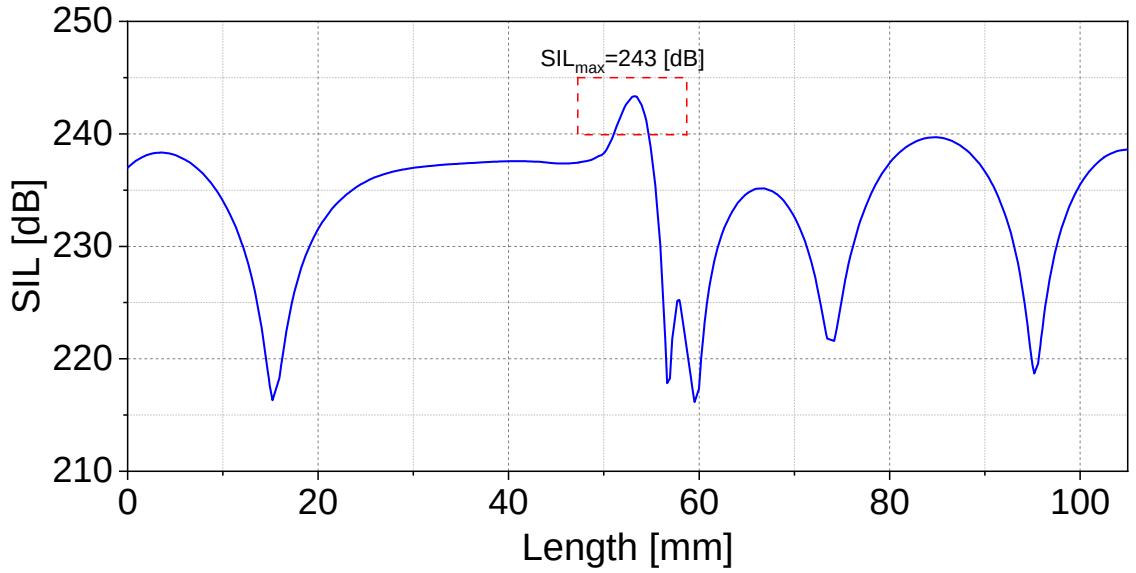

Figure 6. Sound intensity level (SIL) distribution along the central propagation axis at 40 kHz.

Following the two- and three-dimensional characterization of the acoustic pressure field, which enabled the identification of the resonant condition at 40 kHz and the spatial localization of acoustic energy within the *Cucurbita pepo* seed domain, the numerical framework was subsequently extended through a fully coupled thermo-acoustic formulation. The acoustic model was integrated with the *Heat transfer* module to quantify the temperature gradients generated by ultrasonic energy absorption within both the biological matrix and the surrounding aqueous medium.

To ensure strict consistency with the experimental configuration, simulations were conducted under a static pressure of 1.5 MPa, corresponding to the operating conditions of the ultrasonic bath employed during the germination assays. A time-dependent analysis was performed over the interval t = 0–40 min, with an initial uniform temperature of 20 °C, representing the mean ambient temperature at which the experimental treatments were carried out. This temporal window was defined based on the ultrasonic treatment durations applied experimentally (5–25 min), allowing the evaluation of

 doi:10.20944/preprints202602.1926.v1

temperature evolution at each exposure time and the assessment of cumulative thermal effects beyond the maximum treatment period.

The thermo-acoustic coupling accounts for the conversion of acoustic energy into heat through absorption and viscous dissipation mechanisms, enabling the computation of spatially resolved and temporally evolving thermal fields. This approach allows verification that resonance-enhanced ultrasonic exposure at 40 kHz does not induce detrimental thermal loads that could compromise seed viability. Figure 7 presents the temporal temperature dynamics in both the seed and the aqueous medium, illustrating the differential thermal response under sustained ultrasound irradiation.

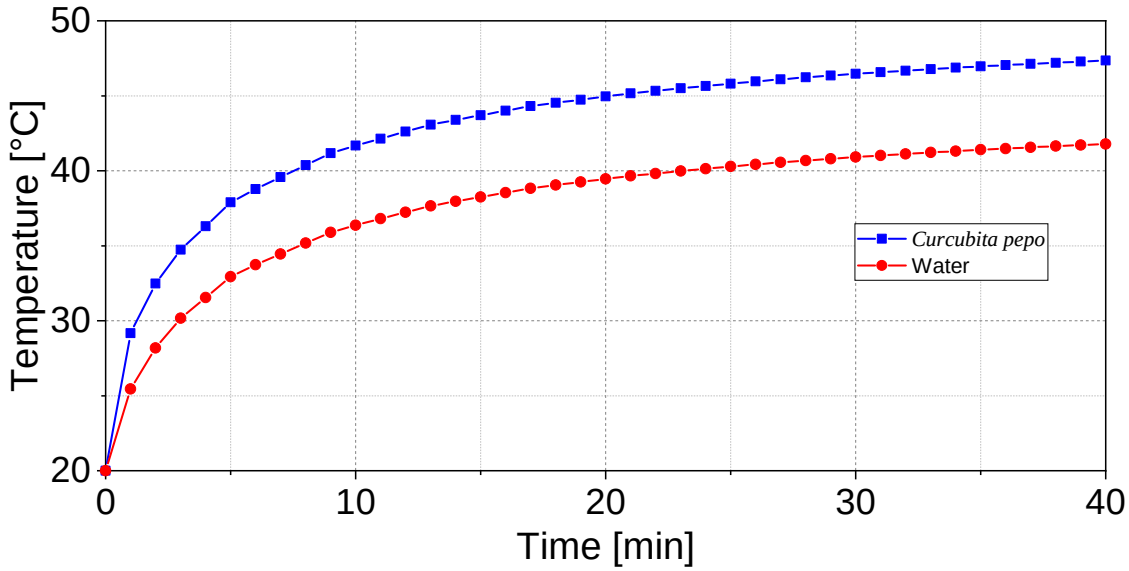

Figure 7. Temporal temperature dynamics of *Cucurbita pepo* seeds and the surrounding water during ultrasonic exposure at 40 kHz.

As shown in Figure 7, the temporal evolution of the thermally induced gradients generated by ultrasonic irradiation at 40 kHz is observed over the interval t= 0–40 min, both within the *Cucurbita pepo* seed domain and in the surrounding aqueous propagation medium. The results reveal a progressive and spatially continuous temperature increase, consistent with the cumulative absorption of acoustic energy and its conversion into heat through viscous and relaxation mechanisms accounted for in the coupled thermo-acoustic model.

Within the seed domain, the temperature rises monotonically from the initial condition of 20 °C at t= 0 to approximately 48 °C at t= 40 min under sustained ultrasonic exposure. The heating profile exhibits a rapid initial increase during the first minutes of irradiation, followed by a gradual attenuation in the rate of temperature rise as conductive and convective heat dissipation mechanisms toward the surrounding medium become more significant. This behavior reflects the balance between localized acoustic energy deposition at resonance and thermal diffusion across the seed–water interface.

Importantly, when the analysis is restricted to the ultrasonic stimulation times implemented experimentally (5, 10, 15, 20, and 25 min), the predicted temperatures remain well below thresholds associated with thermally induced loss of seed viability. Specifically, the seed temperature reaches 37.8 °C at 5 min, 41.6 °C at 10 min, 43.7 °C at 15 min, 44.9 °C at 20 min, and 45.8 °C at 25 min. These values are significantly lower than the critical thermal range reported to induce irreversible damage in plant embryonic tissues, typically above 60 °C. Therefore, under the resonant ultrasonic conditions evaluated, the thermal load imposed on the biological matrix remains within a physiologically safe regime.

Regarding the propagation medium, the maximum temperature attained in the surrounding water was 41.6 °C, indicating a lower thermal accumulation compared to the seed interior. This difference is

 doi:10.20944/preprints202602.1926.v1

attributed to the higher volumetric heat capacity and enhanced thermal dissipation capacity of the aqueous medium, which acts as a heat sink, moderating localized temperature elevations generated at the seed surface. The spatial gradients observed between the seed and the medium further confirm that the dominant energy absorption occurs within the resonant biological domain rather than uniformly in the fluid.

While the previous analysis quantitatively describes the temporal evolution of the temperature field, a spatially resolved interpretation is required to fully characterize the thermo-acoustic behavior of the system. Figure 8 presents the two- and three-dimensional distributions of the temperature field generated under resonant ultrasonic excitation at 40 kHz, providing a detailed visualization of the spatial gradients and the geometric confinement of thermal energy within the *Cucurbita pepo* seed and its surrounding aqueous medium.

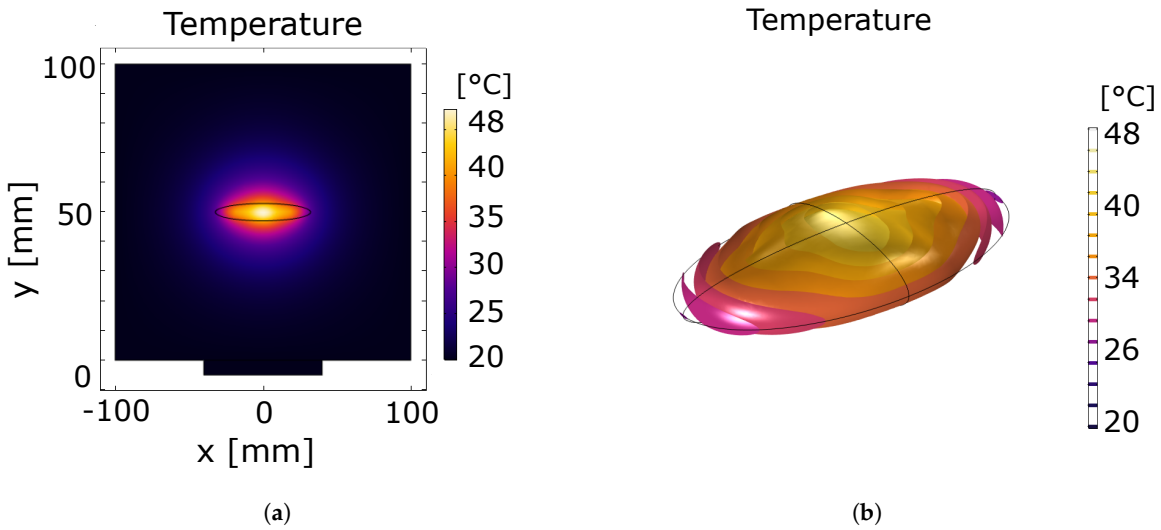

(**a**) (**b**)

Figure 8. Spatial localization of the acoustic field at 40 kHz within the ultrasonic system. (a) 2D intensity distribution; (b) 3D acoustic energy concentration in the seed structure.

Figure 8 provides a spatially resolved visualization of the temperature distribution induced by resonant ultrasonic excitation at 40 kHz through complementary two- and three-dimensional representations. In the 2D cross-sectional map (Figure 8(**a**)), the temperature field is depicted using a chromatic scale ranging from dark blue (≈ 20 °C) to bright yellow–white tones (≈ 45-48 °C). The surrounding aqueous medium is predominantly characterized by dark blue and violet shades, indicating temperatures close to the initial condition and evidencing limited bulk heating. In contrast, the central region corresponding to the seed domain exhibits a progressive transition from blue to green, orange, and finally yellow hues toward its core, revealing a well-defined radial thermal gradient. The highest temperatures are localized in the central axis of the seed, coinciding with the region of maximum acoustic energy concentration previously identified in the pressure field analysis. This distribution indicates that heat generation is spatially confined and directly correlated with resonance-enhanced acoustic absorption rather than uniformly distributed throughout the medium.

The three-dimensional rendering (Figure 8(**b**)), which complements the 2D cross-sectional representation, exclusively depicts the thermal gradients developed within the seed structure, thereby isolating the biological domain from the surrounding aqueous medium. The volumetric visualization reveals an ellipsoidal temperature distribution spanning from approximately 20 °C in the outermost layers to peak values approaching 48 °C in the central core, according to the color scale. Warmer tones (orange to yellow), corresponding to temperatures above 44–48 °C, are concentrated in the inner region of the seed, whereas comparatively cooler hues (pink to light violet, ∼ 30–36 °C) dominate the peripheral zones. This spatial configuration confirms that thermal accumulation is not homogeneous but instead follows the localized pattern of acoustic energy density previously identified under resonant

 doi:10.20944/preprints202602.1926.v1

conditions. The temperature progressively decreases from the central resonant region toward the seed surface, where conductive heat transfer toward the surrounding water facilitates thermal dissipation and stabilizes the overall thermal field.

Collectively, these spatial representations confirm that ultrasonic-induced heating remains geometrically confined to the seed domain, exhibiting well-defined and smoothly distributed thermal gradients without evidence of diffuse or uncontrolled heat propagation into the surrounding aqueous medium. The temperature magnitudes and their spatial distribution are fully consistent with the temporal evolution previously reported, reinforcing the internal coherence of the coupled thermo-acoustic model. Under the applied resonant operating conditions, the resulting thermal field is therefore characterized by localized energy deposition, controlled spatial confinement, and stable heat dissipation toward the propagation medium.

3.2. Baseline Germination Performance

The germination kinetics of non-sonicated *Cucurbita pepo* seeds under controlled environmental conditions are presented in Figure 9. The control group exhibited a markedly limited germination performance throughout the 15-day experimental period. Germination onset was first detected on day 10, reaching approximately 3%, followed by a gradual increase to 10% on day 11 and 13% on day 12. The maximum germination rate (G_r) attained under untreated conditions was approximately 20%, reached on day 13 and remaining statistically unchanged through day 15, thereby establishing the maximum germination time (t_{max}) at 13 days.

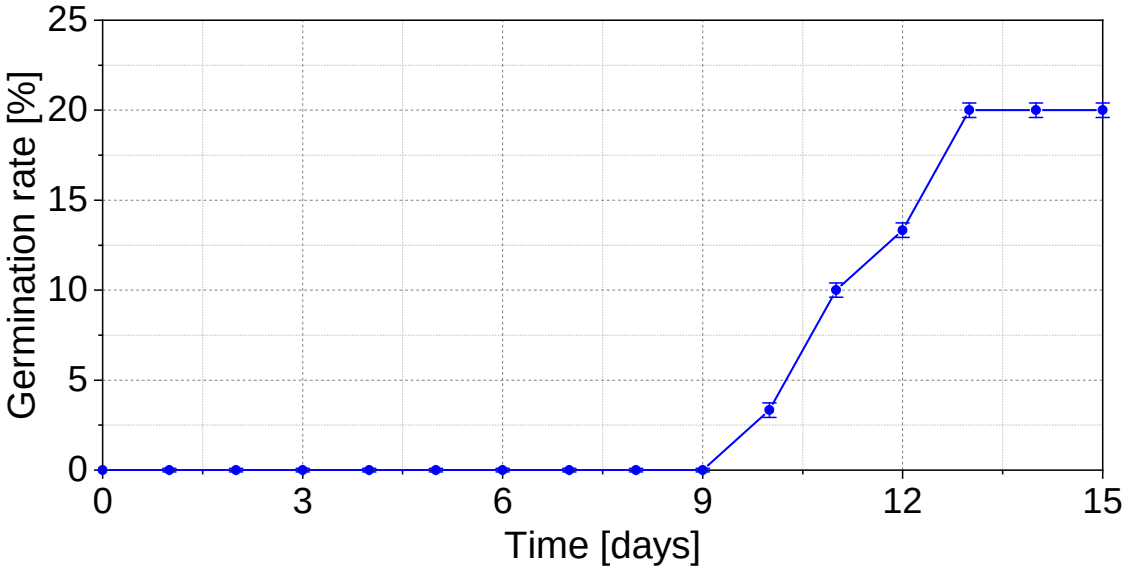

Figure 9. Baseline germination kinetics of untreated *Cucurbita pepo* seeds.

The overall germination index (G_i), calculated as from Eq. 4, yielded a value of approximately 7.8, reflecting low germination vigor and slow emergence dynamics. From a kinetic standpoint, the slope of the germination curve between days 10 and 13 indicates a constrained activation rate, suggesting that intrinsic physical and physiological barriers limit rapid embryo development under baseline conditions.

The relatively low G_r (≈20%) is particularly noteworthy, as it indicates that a substantial fraction of the seed population did not reach the physiological threshold required for cotyledon exposure within the experimental timeframe. Given that environmental variables such as temperature, relative humidity, illumination, and hydration cycles were rigorously controlled, the restricted germination efficiency can be attributed primarily to inherent seed coat permeability constraints and the natural rate of metabolic reactivation.

 doi:10.20944/preprints202602.1926.v1

From a process engineering perspective, these results define a low-efficiency baseline characterized by extended process duration (13 days to reach steady state) and limited conversion of viable seeds into fully germinated seedlings. Such performance highlights the existence of internal mass transfer limitations governing water uptake and subsequent biochemical activation. Consequently, the baseline condition provides a quantitative benchmark against which the degree of process intensification achieved via ultrasound-assisted pre-treatment can be rigorously assessed.

3.3. Ultrasound-Assisted Germination Response

Figure 10 illustrates the germination behavior of *Cucurbita pepo* seeds subjected to increasing ultrasound exposure times compared with the non-ultrasound-treated control (NUST). Ultrasound pre-treatment markedly enhanced germination performance; however, the response exhibited a non-linear dependence on exposure duration.

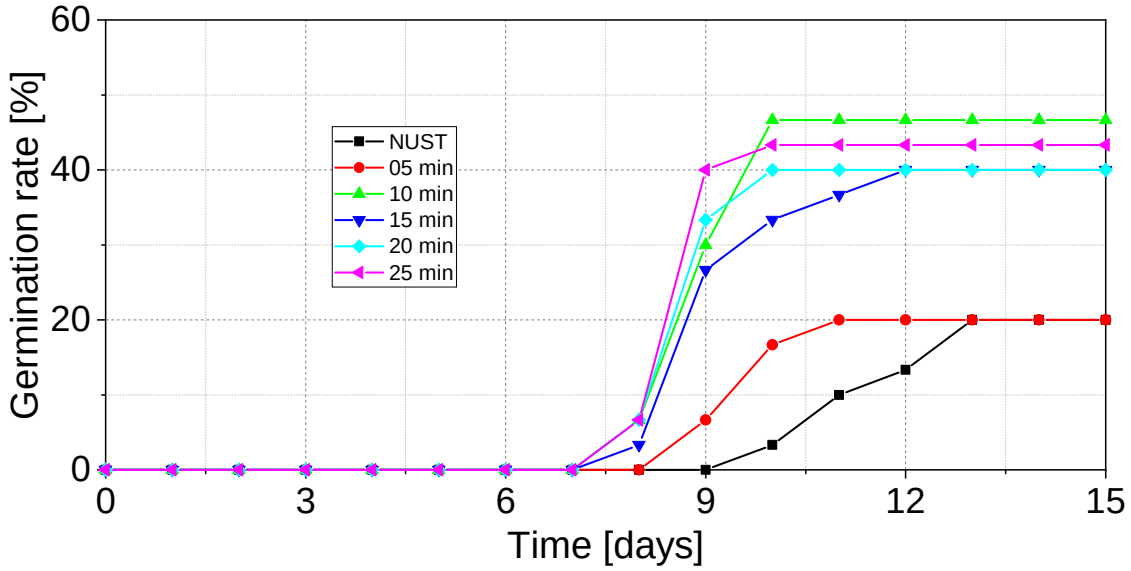

Figure 10. Germination kinetics of *Cucurbita pepo* seeds subjected to ultrasound pre-treatment for 5–25 min compared with non-treated seeds (NUST).

The untreated control reached a G_r of approximately 20% at day 13, displaying slow and limited activation kinetics. In contrast, all ultrasound-treated groups showed earlier germination onset and steeper kinetic slopes.

The 5 min treatment resulted in minimal improvement, reaching a similar final germination percentage (∼20%) as the control, although stabilization occurred slightly earlier. This indicates modest acceleration without enhancement in overall conversion efficiency.

The most pronounced improvement was observed at 10 min of sonication. This treatment achieved the highest G_r (≈47%) by day 10, representing more than a twofold increase relative to the untreated seeds. Additionally, the time required to reach steady state was reduced by approximately three days. The steep slope between days 8 and 10 reflects accelerated metabolic activation and enhanced mass transfer.

The 15 and 20 min treatments both reached a similar final germination percentage of approximately 40%. However, their kinetic profiles differed. The 20 min treatment attained steady state earlier (around day 10–11), whereas the 15 min treatment required approximately one additional day to stabilize. This indicates comparable final efficiency but superior activation kinetics at 20 min. The 25 min treatment achieved a slightly higher final germination (∼43%) but did not surpass the 10 min condition.

 doi:10.20944/preprints202602.1926.v1

The G_i values further confirm these trends. The control exhibited a G_i of approximately 7.8, while the 5 min treatment showed only marginal improvement (≈8.5). Substantial increases were observed for 10, 15, 20, and 25 min treatments, with estimated G_i values of approximately 23, 18, 20, and 19, respectively. Although 15 and 20 min achieved similar G_r values, the higher G_i of the 20 min treatment reflects its faster germination dynamics.

Overall, ultrasound application significantly intensified the germination process by increasing final germination percentage and accelerating activation kinetics. The 10 min treatment emerged as the optimal condition within the evaluated range, providing the highest conversion efficiency and fastest overall germination performance. Longer exposure times maintained enhanced germination relative to the control but did not yield proportional gains, suggesting the existence of an optimal acoustic energy window.

3.4. Water and Energy Consumption Analysis

The germination system operated with a daily electrical consumption of 0.438 kWh and an average daily water consumption of 0.450 L. Because the automated hydration and illumination cycles remained constant across treatments, total resource consumption was directly proportional to the duration required to reach steady-state germination.

Under baseline conditions (NUST), steady state was achieved at day 13, resulting in a total electrical consumption of approximately 5.69 kWh and a cumulative water use of 5.85 L per experimental cycle. This condition therefore represents the reference resource demand associated with conventional, non-assisted germination.

Ultrasound pre-treatment significantly reduced the operational time required to reach germination plateau, leading to proportional reductions in both energy and water consumption. The 10 min treatment, which achieved steady state at day 10, required approximately 4.38 kWh and 4.50 L over the full germination cycle. Relative to the control, this corresponds to a 23% reduction in electrical consumption and a 23% reduction in water use.

The 20 min treatment reached steady state at day 11, with a total consumption of approximately 4.82 kWh and 4.95 L, representing reductions of 15% compared with NUST. In contrast, the 15 min treatment required 12 days to stabilize, resulting in resource consumption comparable to the 5 min condition (approximately 5.26 kWh and 5.40 L). These findings highlight that final germination percentage alone does not determine process sustainability; rather, the combined effect of conversion efficiency and time-to-steady-state governs overall resource intensity.

When resource consumption is evaluated per percentage point of germination achieved, the sustainability advantage of ultrasound becomes even more pronounced. The control consumed approximately 0.285 kWh per percentage point of germination (5.69 kWh / 20%), whereas the 10 min treatment required only approximately 0.093 kWh per percentage point (4.38 kWh / 47%). This represents a nearly threefold improvement in energy efficiency per unit of biological output.

Similarly, water use per percentage point of germination decreased from approximately 0.29 L/% in the control to approximately 0.096 L/% in the 10 min treatment. These results demonstrate that UAG not only accelerates physiological activation but also substantially improves process-level resource efficiency.

From a sustainability perspective, the reduction in operational time directly translates into lower cumulative electricity demand, reduced water throughput, and decreased system occupation time. The identification of an optimal exposure window (10 min) is therefore critical, as excessive sonication does not yield proportional gains and may diminish overall resource efficiency.

Overall, UAG represents a viable process intensification strategy that enhances biological performance while simultaneously reducing energy and water footprints. The integration of kinetic acceleration with measurable reductions in resource consumption supports the potential scalability of this approach within sustainable agricultural and controlled-environment production systems.

 doi:10.20944/preprints202602.1926.v1

4. Discussion

The experimental findings demonstrate that ultrasound pre-treatment significantly intensifies the germination process of *Cucurbita pepo*, enhancing both kinetic performance and final conversion efficiency while simultaneously reducing cumulative resource consumption. Importantly, these biological outcomes are strongly supported by the thermoacoustic multiphysics simulations, which provide a mechanistic and physically grounded explanation for the observed improvements.

The baseline condition (NUST) exhibited limited germination efficiency (≈20%) and required 13 days to reach steady state, reflecting intrinsic mass transfer limitations associated with seed coat permeability and delayed metabolic activation. In contrast, ultrasound exposure at 40 kHz substantially accelerated germination kinetics and increased final germination percentage, with the 10 min treatment achieving ≈47% germination in only 10 days.

The selection of 40 kHz was not arbitrary but derived from frequency-domain spectral analysis identifying this value as the resonance frequency of *Cucurbita pepo* seeds. The multiphysics simulation revealed pronounced acoustic energy localization within the seed domain at resonance, characterized by well-defined pressure nodes and antinodes and maximum sound intensity levels approaching ≈ 243 dB. This spatial concentration of acoustic energy supports enhanced mechanical stimulation at specific structural regions of the seed coat.

Such resonance-driven localization is critical in explaining the non-linear response observed experimentally. At 10 min of exposure, acoustic cavitation and microstreaming likely generate sufficient microstructural perturbations to increase permeability and accelerate imbibition without inducing structural damage. However, as exposure time increases beyond the optimal window, additional mechanical input does not proportionally enhance permeability. The plateau observed at 15 and 20 min suggests that permeability enhancement reaches saturation, after which further energy deposition yields diminishing physiological returns.

The thermo-acoustic coupling further clarifies the mechanism by demonstrating that temperature increases remain within a physiologically safe regime during all experimental exposure times. At 10 min, the predicted seed temperature reached approximately 41.6°C, while even at 25 min it remained below 46°C, well under reported thermal damage thresholds (>60°C). Moreover, spatial temperature distributions confirmed that heating was localized and geometrically confined to the seed domain, with efficient dissipation into the surrounding aqueous medium.

This result is particularly significant because it confirms that the enhanced germination performance cannot be attributed to bulk thermal stimulation. Instead, the dominant mechanism is resonance-enhanced mechanical energy localization, which promotes controlled structural perturbation without inducing detrimental thermal loads. The simulation therefore validates that UAG operates within a mechanically optimized and thermally safe regime.

From a process engineering perspective, the reduction in time-to-steady-state achieved at optimal exposure directly translated into measurable reductions in resource intensity. Because daily energy (0.438 kWh·day^{-1}) and water consumption (0.450 L·day^{-1}) remained constant, shortening the germination period proportionally reduced cumulative demand. The 10 min treatment lowered total electricity consumption by approximately 23% and water use by 23% relative to the control. When normalized per percentage point of germination achieved, energy productivity improved nearly threefold.

The integration of experimental kinetics with thermoacoustic modeling strengthens the robustness of the conclusions. The simulation provides predictive validation of resonance-driven energy localization, while the experimental data confirm its biological efficacy and sustainability benefits. This combined framework exemplifies a rational design approach in which physical modeling informs operational parameter selection, thereby minimizing empirical trial-and-error and improving process efficiency.

Nevertheless, opportunities for further optimization remain. Although 10 min emerged as the optimal exposure under the tested conditions, future studies should evaluate acoustic energy density rather than exposure time alone, enabling scalable parameterization for larger-volume systems. Addi-

 doi:10.20944/preprints202602.1926.v1

tionally, coupling ultrasound with controlled hydration pulses or moderate temperature modulation may further reduce process duration without increasing energy input.

Microstructural characterization techniques such as scanning electron microscopy and permeability assays would also strengthen mechanistic understanding by directly correlating simulated pressure localization with observed structural alterations in the testa. Furthermore, incorporating oxidative stress biomarkers could help determine whether longer exposure times approach physiological stress thresholds.

Overall, the combined experimental and thermoacoustic evidence demonstrates that UAG at the resonance frequency of 40 kHz represents a physically validated and sustainability-oriented process intensification strategy. By aligning acoustic energy localization with biological activation thresholds, the system achieves enhanced germination efficiency, reduced operational duration, and lower cumulative water and electricity footprints. This integrated approach highlights the importance of coupling multiphysics modeling with biological experimentation in the design of resource-efficient agricultural bioprocesses.

5. Conclusions

This study provides quantitative and mechanistic evidence that resonance-driven ultrasound pre-treatment at 40 kHz constitutes a controlled and energy-efficient strategy for intensifying the germination process of *Cucurbita pepo*. By integrating experimental germination kinetics with thermoacoustic multiphysics modeling, the work moves beyond empirical optimization and establishes a physically supported operational framework.

The results demonstrate that a 10 min exposure at the resonance frequency increased final germination from approximately 20% to nearly 48%, representing a 140% enhancement relative to untreated seeds. Simultaneously, the time required to reach steady-state germination decreased from 13 to 10 days, corresponding to a 23% reduction in process duration. Given that daily water (0.450 $L \cdot day^{-1}$) and electrical (0.438 $kWh \cdot day^{-1}$) consumption remained constant across treatments, this kinetic acceleration translated directly into proportional reductions in cumulative resource demand per germination cycle.

Thermoacoustic simulations confirmed that 40 kHz corresponds to a resonance condition that promotes spatial localization of acoustic energy within the seed domain while maintaining temperatures below critical thermal damage thresholds ($<60^{\circ}C$). The absence of excessive bulk heating indicates that germination enhancement is governed primarily by mechanically induced permeability modification rather than thermal stimulation. This distinction is crucial for process design, as it validates ultrasound as a selective physical intensification tool rather than a thermal input mechanism.

Importantly, the data reveal the existence of a finite acoustic energy window. While extended exposure times (15–25 min) maintained improved germination relative to the control, they did not surpass the performance achieved at 10 min, indicating diminishing returns beyond the resonance-optimized duration. This non-linear response underscores the necessity of energy-normalized optimization in ultrasound-assisted bioprocesses and highlights the risk of overexposure without proportional biological benefit.

From a sustainability perspective, the optimal treatment reduced energy and water intensity per percentage point of germination by nearly threefold compared to untreated seeds. Such improvements position resonance-tuned ultrasound as a viable intensification strategy for controlled-environment agriculture, where resource efficiency and process throughput are critical performance metrics.

Overall, this work establishes a reproducible methodology for coupling multiphysics simulation with biological validation to optimize acoustic pre-treatment parameters. The findings contribute to the rational design of low-intensity, resource-efficient germination systems and provide a foundation for future scaling analyses based on acoustic energy density, structural characterization of seed coat modification, and techno-economic assessment.

 doi:10.20944/preprints202602.1926.v1

Author Contributions: Conceptualization, D. Aguilar-Torres, O. Jiménez-Ramírez and R. Vázquez-Medina; Methodology, D. Aguilar-Torres, O. Jiménez-Ramírez; Software, D. Aguilar-Torres; Validation, D. Aguilar-Torres, O. Jiménez-Ramírez, and R. Vázquez-Medina; Formal analysis, D. Aguilar-Torres, and O. Jiménez-Ramírez; Investigation, D. Aguilar-Torres and F. A. Perdomo; Resources, O. Jiménez-Ramírez and R. Vázquez-Medina; Data curation, F. A. Perdomo; Writing—original draft preparation, D. Aguilar-Torres and R. Vázquez-Medina; Writing—review and editing, D. Aguilar-Torres, F. A. Perdomo, O. Jiménez-Ramírez and R. Vázquez-Medina; Visualization, D. Aguilar-Torres and F. A. Perdomo; Supervision, R. Vázquez-Medina and O. Jiméz-Ramírez.; Project administration, R. Vázquez-Medina; Funding acquisition, R. Vázquez-Medina, and O. Jiménez-Ramírez. All authors have read and agreed to the published version of the manuscript.

Funding: This research was funded by Instituto Politécnico Nacional [Grant numbers: SIP-20250154 (O. Jiménez-Ramírez)], and SIP-20250150, SIP-20250321 (R. Vázquez-Medina)].

Institutional Review Board Statement: Not applicable.

Informed Consent Statement: Not applicable.

Data Availability Statement: Dataset available on request from the authors.

Acknowledgments: D. Aguilar-Torres (CVU-829790) is grateful for the grant provided by Secretaría de Ciencia, Humanidades, Tecnología e Innovación (SECIHTI, Mexico)

Conflicts of Interest: The authors declare no conflict of interest.

Abbreviations

The following abbreviations are used in this manuscript:

UAG	Ultrasound–assisted germination
ABA	Abscisic acid
ET	Ethylene
JA	Jasmonate
G_{max}	Maximum germination capacity
λ	Lag phase
FEM	Finit element method
2D	Two dimensions
3D	Three dimensions
PET	Polyethylene Terephthalate
G_r	Germination rate
G_i	Germination index
E	Total energy input
SIL	Sound Intensity Level
t_{max}	Maximum germination time
NUST	Non-ultrasound-treated

References

1. Bewley, J.D.; Bradford, K.J.; Hilhorst, H.W.; Nonogaki, H. *Seeds:Physiology of Development, Germination and Dormancy, 3rd Edition*; Springer New York, 2013. https://doi.org/10.1007/978-1-4614-4693-4.
2. Paparella, S.; Araújo, S.S.; Rossi, G.; Wijayasinghe, M.; Carbonera, D.; Balestrazzi, A. Seed priming: state of the art and new perspectives. *Plant Cell Reports* **2015**, *34*, 1281–1293. https://doi.org/10.1007/s00299-015-1784-y.
3. Farooq, M.; Wahid, A.; Siddique, K.H.M. Micronutrient application through seed treatments: a review. *Journal of soil science and plant nutrition* **2012**, *12*, 125–142. https://doi.org/10.4067/s0718-95162012000100011.
4. Aguilar-Torres, D.; Jiménez-Ramírez, O.; Perdomo, F.; Vázquez-Medina, R. Advanced Sustainable Food Processing: Ultrasound-Assisted Germination of Cucurbita pepo Seeds. In Proceedings of the The 4th International Electronic Conference on Processes session Food Process Engineering. MDPI, 2025.
5. Mason, T.J.; Lorimer, J.P. *Applied Sonochemistry: Uses of Power Ultrasound in Chemistry and Processing*; Wiley, 2002. https://doi.org/10.1002/352760054x.

 doi:10.20944/preprints202602.1926.v1

6. Rifna, E.; Ratish Ramanan, K.; Mahendran, R. Emerging technology applications for improving seed germination. *Trends in Food Science & Technology* **2019**, *86*, 95–108. https://doi.org/10.1016/j.tifs.2019.02.029.
7. GOUSSOUS, S.J.; SAMARAH, N.H.; ALQUDAH, A.M.; OTHMAN, M.O. ENHANCING SEED GERMINATION OF FOUR CROP SPECIES USING AN ULTRASONIC TECHNIQUE. *Experimental Agriculture* **2010**, *46*, 231–242. https://doi.org/10.1017/s0014479709991062.
8. Yaldagard, M.; Mortazavi, S.A.; Tabatabaie, F. Influence of ultrasonic stimulation on the germination of barley seed and its alpha-amylase activity. *African Journal of Biotechnology* **2008**, *7*.
9. Nogueira, A.; Teixeira, A.; Gerós, H.; Puga, H. Ultrasound Prototype for Improving Germination and Seedling Growth in Tomato and Maize Seeds. *Journal of Plant Growth Regulation* **2023**, *43*, 1216–1229. https://doi.org/10.1007/s00344-023-11178-7.
10. Gong, M.; Kong, M.; Huo, Q.; He, J.; He, J.; Yan, Z.; Lu, C.; Jiang, Y.; Song, J.; Han, W.; et al. Ultrasonic treatment can improve maize seed germination and abiotic stress resistance. *BMC Plant Biology* **2024**, *24*. https://doi.org/10.1186/s12870-024-05474-x.
11. Nogueira, A.; Puga, H.; Gerós, H.; Teixeira, A. Ultrasound-enhanced seed hydration: impacts on seedling vigor, gene expression and absorption kinetics in maize, bean and pepper seeds. *Journal of the Science of Food and Agriculture* **2025**, *105*, 7227–7241. https://doi.org/10.1002/jsfa.14426.
12. Huang, S.; Ashraf, U.; Duan, M.; Ren, Y.; Xing, P.; Yan, Z.; Tang, X. Ultrasonic seed treatment improved seed germination, growth, and yield of rice by modulating associated physio-biochemical mechanisms. *Ultrasonics Sonochemistry* **2024**, *104*, 106821. https://doi.org/10.1016/j.ultsonch.2024.106821.
13. Nogueira, A.; Puga, H.; Gerós, H.; Teixeira, A. Seed germination and seedling development assisted by ultrasound: gaps and future research directions. *Journal of the Science of Food and Agriculture* **2023**, *104*, 583–597. https://doi.org/10.1002/jsfa.12994.
14. Király, A.; Farkas, D.; Dobránszki, J. Ultrasound in Plant Life and Its Application Perspectives in Horticulture and Agriculture. *Horticulturae* **2025**, *11*, 318. https://doi.org/10.3390/horticulturae11030318.
15. Alfalahi, A.O.; Alobaidy, B.S.; Almarie, A.A.; Dhanoon, O.M.; Qasem, J.R.; Almehemdi, A.F.; Najda, A. Ultrasonic Treatment Enhances Germination and Affects Antioxidant Gene Expression in Soybean (Glycine max L. Merr). *Agronomy* **2022**, *12*, 2446. https://doi.org/10.3390/agronomy12102446.
16. Tufail, T.; Ul Ain, H.B.; Ashraf, J.; Saeed, F.; Basharat, Z.; Ahmed, Z.; Waseem, M.; Xu, B.; Manzoor, M.F.; Mugabi, R. Effects of germination and ultrasound treatment on the thermodynamics, nutritional and structural quality of highland barley fractions. *Ultrasonics Sonochemistry* **2025**, *123*, 107652. https://doi.org/10.1016/j.ultsonch.2025.107652.
17. Villamiel, M.; García-Pérez, J.V.; Montilla, A.; Carcel, J.A.; Benedito, J. Ultrasound in food processing: Recent advances. *Wiley Blackwell* **2017**.
18. Dhatt, A.; Pandey, S.; Garch, K.S.; Verma, N.; Sagar, V.; Sharma, M. Comprehensive review of pumpkin (Cucurbita spp.): Domestication, global distribution, genetic characterization, breeding strategies, and genomic insights. *Vegetable Science* **2024**, *51*. https://doi.org/10.61180/vegsci.2024.v51.i2.01.
19. Paris, H.S. Historical records, origins, and development of the edible cultivar groups of Cucurbita pepo (Cucurbitaceae). *Economic Botany* **1989**, *43*, 423–443. https://doi.org/10.1007/bf02935916.
20. Decker, D.S. Origin(s), evolution, and systematics of Cucurbita pepo (Cucurbitaceae). *Economic Botany* **1988**, *42*, 4–15. https://doi.org/10.1007/bf02859022.
21. Foschi, M.L.; Juan, M.; Pascual, B.; Pascual-Seva, N. Effects of High Intensity Ultrasound Stimulation on the Germination Performance of Caper Seeds. *Plants* **2023**, *12*, 2379. https://doi.org/10.3390/plants12122379.
22. Qin, Q.; Zhang, L.; Yin, H.; Yu, J.; Hu, S.; Zhang, Z.; Liu, J. Enhancing malting performance of harder barley varieties through ultrasound treatment. *Ultrasonics Sonochemistry* **2024**, *105*, 106860. https://doi.org/10.1016/j.ultsonch.2024.106860.
23. Ramos-Pacheco, B.S.; Peralta-Guevara, D.E.; Yauris-Silvera, C.R.; Medina-Gutierrez, C.A.; Loayza-Buleje, J.J. Ultrasound-Assisted Germination: Impact of Time and Frequency on the Physical, Chemical, Thermal Properties and Bioactive Compounds of High Andean Quinoa. *Processes* **2025**, *14*, 98. https://doi.org/10.3390/pr14010098.
24. Rashid, M.T.; Liu, K.; Muzaffar, N.; Alohali, B.M.; Jatoi, M.A.; Usman, H.; Aadil, R.M. Impact of ultrasound-assisted germination and varied drying methods on phenolic biosynthesis, antioxidant capacity, and oxidative enzyme activity in selenium-biofortified black rice. *Ultrasonics Sonochemistry* **2025**, *123*, 107692. https://doi.org/10.1016/j.ultsonch.2025.107692.

 doi:10.20944/preprints202602.1926.v1

25. dos Santos, M.A.; Pacheco, F.C.; Gusmão, M.H.A.; Andressa, I.; Pacheco, A.F.C.; Paiva, P.H.C.; Gomes, F.T. Ultrasound-assisted Hydration Improves Germination and Early Growth of Moringa oleifera Under Salinity Stress. *Journal of Soil Science and Plant Nutrition* **2026**. https://doi.org/10.1007/s42729-025-02978-9.
26. Macedo, C.; Silva, A.M.; Ferreira, A.S.; Moreira, M.M.; Delerue-Matos, C.; Rodrigues, F. Microwave- and Ultrasound-Assisted Extraction of Cucurbita pepo Seeds: A Comparison Study of Antioxidant Activity, Phenolic Profile, and In-Vitro Cells Effects. *Applied Sciences* **2022**, *12*, 1763. https://doi.org/10.3390/app12031763.
27. Iglesias-Moya, J.; Cebrián, G.; Garrido, D.; Martínez, C.; Jamilena, M. The ethylene receptor mutation etr2b reveals crosstalk between ethylene and ABA in the control of Cucurbita pepo germination. *Physiologia Plantarum* **2023**, *175*. https://doi.org/10.1111/ppl.13864.
28. Acila, S.; Derouiche, S.; Allioui, N. Embryo growth alteration and oxidative stress responses in germinating Cucurbita pepo seeds exposed to cadmium and copper toxicity. *Scientific Reports* **2024**, *14*. https://doi.org/10.1038/s41598-024-58635-1.
29. Irik, H.A.; Bikmaz, G. Effect of different salinity on seed germination, growth parameters and biochemical contents of pumpkin (Cucurbita pepo L.) seeds cultivars. *Scientific Reports* **2024**, *14*. https://doi.org/10.1038/s41598-024-55325-w.
30. Alonso, S.; Gautam, K.; Iglesias-Moya, J.; Martínez, C.; Jamilena, M. Crosstalk between Ethylene, Jasmonate and ABA in Response to Salt Stress during Germination and Early Plant Growth in Cucurbita pepo. *International Journal of Molecular Sciences* **2024**, *25*, 8728. https://doi.org/10.3390/ijms25168728.
31. Liang, L.; Chen, L.; Liu, G.; Zhang, F.; Linhardt, R.J.; Sun, B.; Li, Q.; Zhang, Y. Optimization of germination and ultrasonic-assisted extraction for the enhancement of aminobutyric acid in pumpkin seed. *Food Science & Nutrition* **2022**, *10*, 2101–2110. https://doi.org/10.1002/fsn3.2826.
32. Pacheco, F.C.; Cunha, J.S.; Andressa, I.; dos Santos, F.R.; Pacheco, A.F.C.; Nalon, G.A.; Paiva, P.H.C.; Tribst, A.A.L.; Augusto, P.E.D.; Leite Júnior, B.R.d.C. Ultrasound-Assisted Intermittent Hydration of Pumpkin Seeds: Improving the Water Uptake, Germination, and Quality of a Clean Label Ingredient. *Food and Bioprocess Technology* **2024**, *18*, 618–632. https://doi.org/10.1007/s11947-024-03487-w.
33. Blackstock, D.T. *Fundamentals of physical acoustics*; John Wiley & Sons, 2000.
34. Aguilar-Torres, D.; Jiménez-Ramírez, O.; Hernández-Gama, R.; Perdomo-Hurtado, F.A.; Vázquez-Medina, R. Multiphysics analysis for ultrasound settings that can disinfect food: Inactivation of E. coli in apples. *Food Control* **2025**, *172*, 111191. https://doi.org/10.1016/j.foodcont.2025.111191.
35. Aguilar-Torres, D.; Jiménez-Ramírez, O.; Camacho-Martínez, J.L.; Vázquez-Medina, R. Multiphysics analysis of a high-intensity ultrasound system applied to a three-layer animal tissue. *WFUMB Ultrasound Open* **2024**, *2*, 100039. https://doi.org/10.1016/j.wfumbo.2024.100039.
36. Prinn, A.G. A Review of Finite Element Methods for Room Acoustics. *Acoustics* **2023**, *5*, 367–395. https://doi.org/10.3390/acoustics5020022.
37. Ranal, M.A.; Santana, D.G.d. How and why to measure the germination process? *Revista Brasileira de Botânica* **2006**, *29*, 1–11. https://doi.org/10.1590/s0100-84042006000100002.
38. Chiapusio, G.; Sánchez, A.M.; Reigosa, M.J.; González, L.; Pellissier, F. Do Germination Indices Adequately Reflect Allelochemical Effects on the Germination Process? *Journal of Chemical Ecology* **1997**, *23*, 2445–2453. https://doi.org/10.1023/b:joec.0000006658.27633.15.